Multimodal droplet barcoding enables high-throughput linking of single-cell imaging and gene expression

Catherine K Xu[1,2*], Georg Meisl[3], Nikita Moshkov[4], Niklas A Schmacke[4], Karolis Goda[5], Alexey Shkarin[1], Maximilian F Schlögel[1], Tuomas PJ Knowles[3,6], Fabian J Theis[4,7,8], Linas Mazutis[5], Jochen Guck[1,2†]

To whom correspondence should be addressed: cathxu@ethz.ch

[†]Deceased

[1]Max Planck Institute for the Science of Light, Erlangen, Germany

[2]Max Planck Zentrum für Physik und Medizin, Erlangen, Germany

[3]Yusuf Hamied Department of Chemistry, University of Cambridge, Cambridge, UK

[4]Institute of Computational Biology, Helmholtz Munich, Munich, Germany

[5]Institute of Biotechnology, Vilnius University, Vilnius, Lithuania

[6]Cavendish Laboratory, University of Cambridge, Cambridge, UK

[7]TUM School of Life Sciences Weihenstephan, Technical University of Munich, Munich, Germany

[8]School of Computation, Information and Technology, Technical University of Munich, Munich, Germany

Abstract

Understanding sequence-function relationships in biology requires large-scale datasets that provide one-to-one mapping between sequence and phenotype. Here, we address this challenge by introducing multimodal droplet barcoding, a strategy that enables individual microfluidic droplets to be tracked across both optical and sequencing measurements. We demonstrate the power of this approach through

single-cell analysis, linking single-cell imaging with gene expression profiling at throughputs of hundreds of cells per minute.

Main text

A central challenge in biology is how function arises from sequence, whether at the level of protein molecules or cells. Elucidating this relationship requires large amounts of data linking the modalities of functionality and sequence. Droplet microfluidics provides an attractive solution where, by compartmentalising reactions in pico- to nanolitre-scale droplets, we can achieve orders of magnitude higher throughputs than macro-level experiments. This has been harnessed extensively in areas including high-throughput single-cell mRNA sequencing (scRNA-seq) and protein function screening [1, 2, 3]. However, the true potential of droplets has not yet been realised: unlike in macro-scale experiments, we cannot link multiple measurements at the single-droplet level at scale. This severely limits opportunities to disentangle the sequence-function relationship.

Current strategies to link microfluidic measurements across modalities rely on sorting, arrays, or high-precision handling. Sorting droplets into "positive" and "negative" populations is extremely powerful for directed evolution, but reduces optical phenotype measurements to a one-dimensional binary readout [3, 4]. Static, array-based approaches are inherently limited in throughput and scalability [5, 6, 7, 8, 9, 10]. High-precision handling is required in deterministic flow-based systems which precisely control individual cells or droplets, ultimately limiting their analysis rate [11, 12, 13].

Here, we developed multimodal droplet barcoding as strategy to address this challenge. We tag each droplet with a unique barcode readable in multiple modalities, enabling high-throughput, multimodal measurements which we demonstrate for single-cell analysis. Rather than enforcing determinism, we deliberately harness randomness to generate unique, multimodal barcodes for droplets. Large numbers of hydrogel beads with unique DNA barcodes can be easily constructed by combinatorial DNA extension, but these beads are optically identical [1, 14, 15]. Synthesising a unique, optically distinct, DNA-labelled barcode bead for each droplet is not scalable. We therefore employ a combinatorial strategy, whereby optically identifiable, DNA-labelled beads are randomly combined to generate multi-

component barcodes [9, 16, 17]. This combinatorial approach scales extremely well, with just 30 such multimodal barcode (MB) beads able to yield over 1 billion composite barcodes. Given limitations on the number of MB beads per droplet barcode, we synthesised 41 unique MB bead types by varying their size, shape, and colour (Figure 2a-d), and reversibly conjugated each type to a unique, known DNA sequence [17, 18, 19]. MB component beads can be identified in droplets both optically and by sequencing, to yield the complete barcode (Figure 2b).

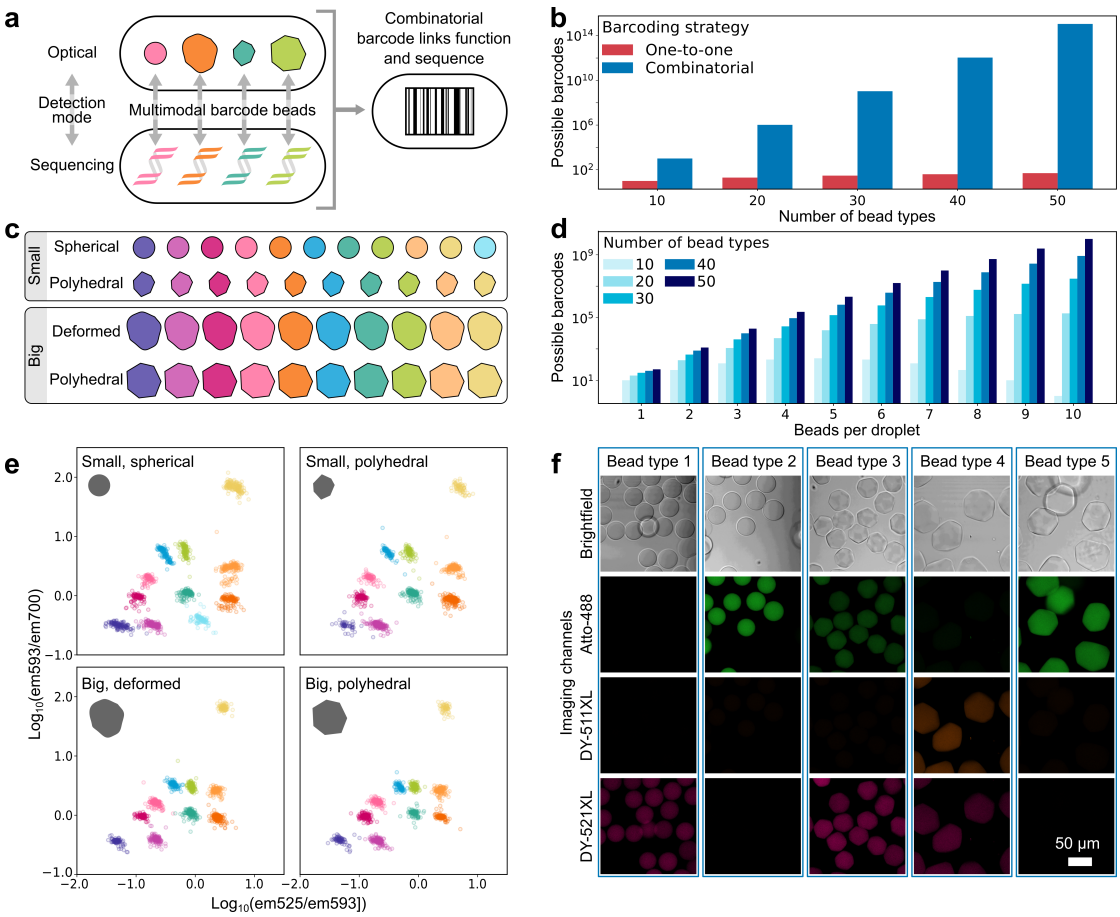

Figure 1: **Generation of multimodal barcodes.** (**a**) Multimodal barcodes are generated by the random combination of multimodal barcode (MB) beads, each of which is identifiably both optically and by sequencing. (**b**) This combinatorial approach is extremely scalable: from just 30 types of multimodal barcode beads, over 1 billion barcodes can be generated. (**c**) Schematic representation of the 41 MB bead types used in this study, using the parameters of size, colour, and shape to render them optically distinct. (**d**) The number of barcodes depends on the number of MB beads per droplet. With 41 MB bead types, millions of barcodes are possible even if the number of beads per droplet is capped at 6. (**e**) Ratiometric bead colours defined by the combination of three fluorescent dyes. The three fluorescence signals (emission at 525, 593, and 700 nm) were reduced to two axes by taking the pairwise ratios, removing noise arising from variations in absolute fluorescence intensity. Colours are shown for the four size/shape combinations. (**f**) Example brightfield and fluorescence images of types (columns) of multimodal barcode beads.

Having established the construction of multimodal droplet barcodes, we demonstrated their application to single-cell analysis. We designed our MB beads to directly integrate into existing scRNA-seq methods, to add the additional dimension of cell imaging. Despite the abundance of technologies for single-cell interrogation, multimodal characterisation is sparse and yet increasingly recognised as crucial for providing both insights into inter-modality relationships and foundations for integrating single-modality datasets [20, 21, 22, 23]. In contrast to spatial omics methods requiring fixation, microfluidic characterisation is compatible with live cells and can thus access cell properties such as mechanical stiffness and secretion, and do so in a time-resolved manner [24, 25, 26].

In droplet-based scRNA-seq, single cells are co-encapsulated with uniquely DNA-barcoded beads (blind barcode beads) which index sequences during reverse transcription [1, 2, 14]. Our platform, im-seq, images live cells directly prior to their encapsulation in droplets. In addition to blind barcode beads, droplets now also contain MB beads. The blind barcode bead then tags both MB-derived DNA and cell mRNA with the same unique sequence [27, 28]. The combinatorial multimodal barcode thereby links optical and sequencing data at the single-cell level (Figure 2).

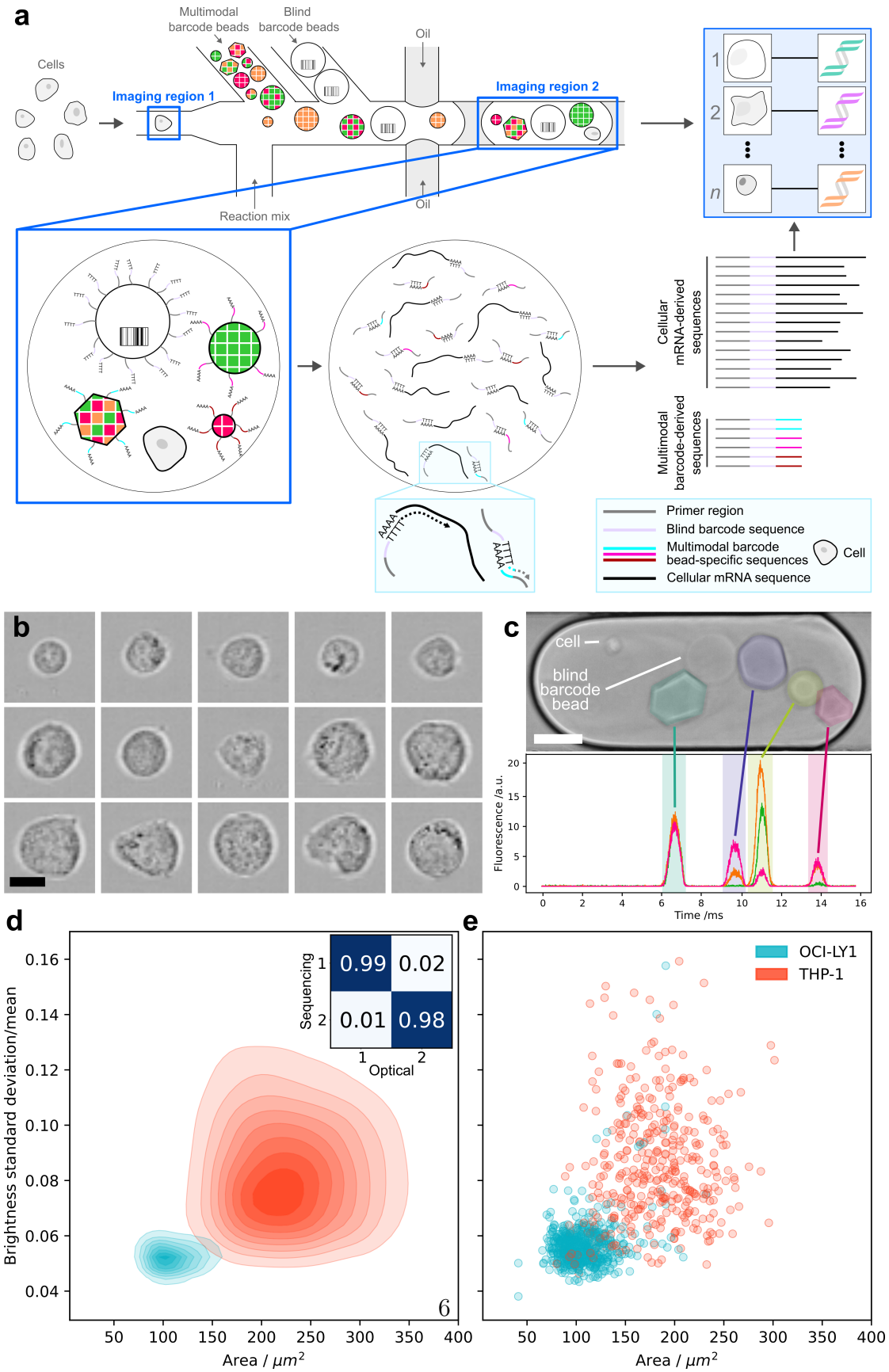
a
Cells
Multimodal barcode beads
Blind barcode beads
Oil
Imaging region 1
Imaging region 2
Reaction mix
Oil
1
2
n
Cellular mRNA-derived sequences
Multimodal barcode-derived sequences
Primer region
Blind barcode sequence
Multimodal barcode bead-specific sequences
Cellular mRNA sequence
Cell
b
c
cell
blind barcode bead
Fluorescence /a.u.
Time /ms
d
Brightness standard deviation/mean
Area / μm²
Sequencing
Optical
0.99
0.02
0.01
0.98
e
OCI-LY1
THP-1
Area / μm²

Figure 2: **Multimodal barcodes link single-cell image and gene expression.** (**a**) Schematic of high-throughput, multimodal single-cell analysis by barcoding. Live cells are imaged (imaging region 1) immediately prior to encapsulation with both blind barcode beads and multimodal barcode beads. The multimodal barcode beads, which are functionalised with known DNA sequences, enable direct image-to-transcriptome linking of single cells. (**b**) Example images of cells (imaging region 1) immediately prior to encapsulation in droplets. Scale bar: 10 µm. (**c**) Droplet containing a cell, blind barcode bead, and four multimodal component beads which comprise the multimodal barcode. Fluorescence traces determine the colour of each bead (coloured as in Figure 1(**e**)) (Scale bar: 50 µm.). (**d**) OCI-LY1 (turquoise) and THP-1 (orange) cells were imaged in separate measurements, showing distinct physical properties. Inset: ground truth validation of linking optical and sequencing data, by combining data from two separate experiments. In >98% of linked droplets, sequencing data were paired with optical droplet data from the same experiment class. (**e**) Plot of image features of 943 OCI-LY1 and THP-1 cells, coloured according to the gene expression-based cell type classification.

To validate that our multimodal barcodes are correctly and uniquely linked between imaging and sequencing data, we mixed data from two experiments. This produced one set of barcoded cell-containing droplets detected optically and another by sequencing, both originating from a mixture of experiment classes 1 and 2. We then analysed these mixed datasets to identify droplets with the same unique barcodes detected in both modalities. Comparison of these linked pairs with the known experiment classes confirmed that over 98% of matched droplets were correctly classified (Figure 2d (inset)), with mismatches likely originating from low signal-to-noise ratios in multimodal barcode bead sequencing for a minority of droplets. We next applied im-seq to a mixture of two cell lines: OCI-LY1 and THP-1, which differ in physical phenotype at the population level (Figure 2f), reproduced by cell type classification based on mRNA expression (Figure 2e). While just two representative image-based parameters are displayed here, the dataset for each cell contains the whole image (Figure 2b).

We next explored gene expression–feature relationships in haematopoietic cell lines (HL-60, THP-1, and OCI-LY1). From the cell images, we extracted morphologi-

cal parameters and interrogated associated transcriptional programmes, observing clearer separation between cell lines in gene-expression space than in image-feature space (Figure 3a, b) [29]. Annotating gene-expression embeddings with cellular imaging-derived properties demonstrated that detailed cell state descriptions require both imaging and gene expression data (Figure 3c, d).

Cell size differed substantially both across and within cell lines and thus serves as an easily interpretable showcase for linking image features to gene expression (Figure 3e). Correlation analyses across all cell lines identified both positively and negatively associated transcripts, including actin/cytoskeletal regulators such as CAP1 (positive) and TMSB4X (negative), as well as the cell-cycle inhibitor CDKN2A (negative) [30, 31]. Ribosomal genes were enriched among negatively correlated transcripts, consistent with cell-cycle–dependent regulation of translation, while immune and myeloid-state markers such as CHI3L1, ELANE, and LST1 were enriched among transcripts positively correlated with cell size (Figure 3f) [32, 33, 34, 35]. Closer inspection within cell lines revealed distinct classes of gene–image relationships, including genes whose apparent association is driven primarily by between–cell line differences versus genes that correlate consistently within each line; for example, the proliferation-associated TOP2A showed a positive association with cell size within, but not between, cell lines (Figure 3g-i).

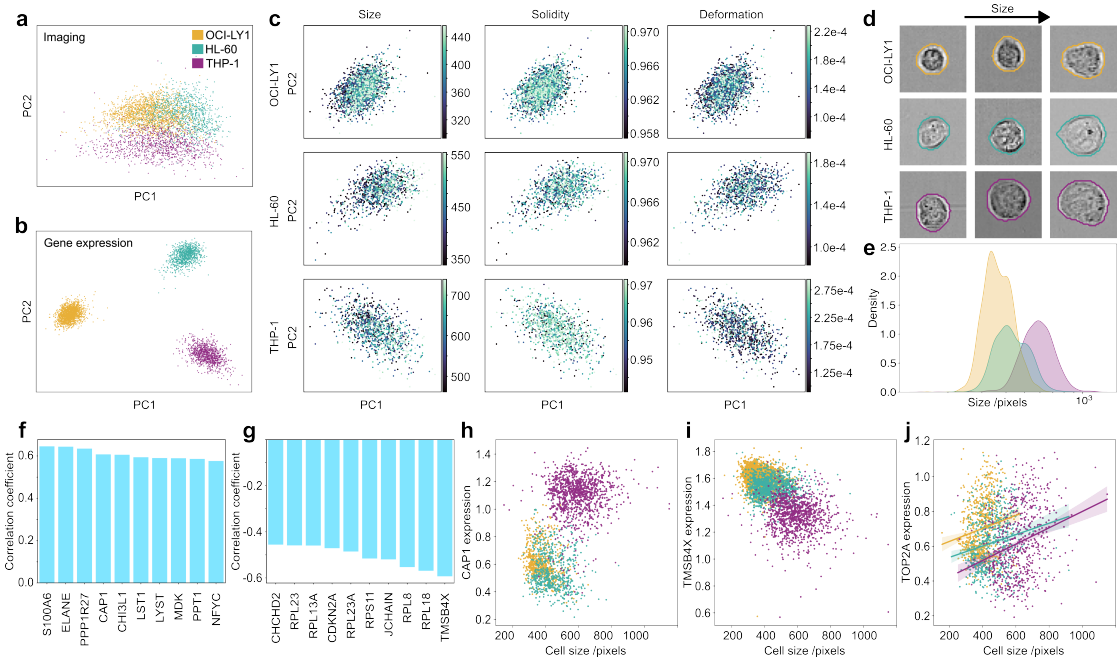

Figure 3: **Gene expression-imaging associations in haematopoietic cell lines** (**a**) Principal component analysis (PCA) of single-cell images of different cell lines acquired by im-seq. Images were featurised with CellProfiler [36]. Colours throughout the figure are yellow: OCI-LY1, turquoise: HL-60, and purple: THP-1. (**b**) PCA of single-cell gene expression in the same datasets as **a**). (**c**) PCA of single-cell gene expression for each cell line, coloured according to the magnitude of the indicated image-derived properties. (**d**) Example single-cell images of different cell lines, sorted according to cell size and shown alongside their segmentation. (**e**) Size distributions of cell lines as measured by im-seq. (**f** and **g**) Genes with the top ten most positively (**f**) and negatively (**g**) correlated expression with cell size across cell lines. (**h-j**) Examples of different types of correlations between cell size and the expression of individual genes observed by im-seq. Gene expression may be correlated across (**h**, **i**) or within (**j**) cell lines.

In conclusion, we present a general strategy for multimodal single-cell characterisation at high throughput, which combines the versatility of optical-based characterisation with the scalability of droplet sequencing workflows. Approaches based on sorting cells into subpopulations discretise inherently continuous features and require that cell states of interest are pre-defined, limiting discovery of unexpected or multi-dimensional relationships. Current single-cell image-transcriptome link-

ing methods are limited in throughput and scalability due to the use of arrays or deterministic control. Our continuous flow-based approach is fast (currently 1000 cells in 5 minutes) and scalable. Moreover, the implementation is relatively simple, requiring only a commercially available microscope and syringe pumps, without complex liquid handling such as valves and controlled cell/droplet dispensing [12, 13, 11, 37].

The multimodal barcoding approach is modular and compatible with a broad range of cell characterisation modalities such as fluorescence imaging flow cytometry [38]. Moreover, the barcodes are compatible with live cells, meaning they can be integrated with functional assays such as time-resolved secretion profiling in droplets [25, 39] and perturbation screens [40, 41, 42], while also avoiding fixation-induced artefacts [24, 43]. We anticipate that multimodal barcoding will open new avenues for studying the relationship between cell phenotypes and gene expression programmes in health and disease.

Acknowledgements

We are grateful to Cornelia Liebers, Manuela Hauke, and Christine Schweitzer for culturing cells, to Dr Irina Harder, Parth Patel, and Dr Salvatore Girardo for their support in the clean room, and to Dr Arif Ekici and Dr Rinho Kim for their support with sequencing. We also thank Dr David Morse, Dr Tomasz Kaminski, and Professor Justus Kebschull for their helpful discussions. This research received funding from: the Peter und Traudl Engelhorn Stiftung fellowship (C.K.X), the HFSP Cross-Disciplinary Fellowship (C.K.X.), the Marie Skłodowska-Curie Actions fellowship READ-seq (agreement no. 101068803) (C.K.X.).

Author contributions

Project conception: C.K.X., G.M., J.G. Experiments: C.K.X., K.G. Software and analysis: C.K.X., G.M., N.M., N.S., M.F.S., T.P.J.K., F.T. Writing (original draft): C.K.X. Writing (reviewing and editing): C.K.X., G.M., N.S., N.M., K.G., A.S., M.F.S., T.P.J.K., F.T., L.M., J.G.

Competing interests

A patent has been filed for the technology (inventors C.K.X., G.M., T.P.J.K., and J.G) by the institutions Cambridge Enterprise and Max Planck Innovation (WO

2025/146377).

References

[1] Allon M. Klein, Linas Mazutis, Ilke Akartuna, Naren Tallapragada, Adrian Veres, Victor Li, Leonid Peshkin, David A. Weitz, and Marc W. Kirschner. Droplet barcoding for single-cell transcriptomics applied to embryonic stem cells. *Cell*, 161(5):1187–1201, May 2015.

[2] Evan Z. Macosko, Anindita Basu, Rahul Satija, James Nemesh, Karthik Shekhar, Melissa Goldman, Itay Tirosh, Allison R. Bialas, Nolan Kamitaki, Emily M. Martersteck, John J. Trombetta, David A. Weitz, Joshua R. Sanes, Alex K. Shalek, Aviv Regev, and Steven A. McCarroll. Highly parallel genome-wide expression profiling of individual cells using nanoliter droplets. *Cell*, 161(5):1202–1214, May 2015.

[3] Ariane Stucki, Jaicy Vallapurackal, Thomas R Ward, and Petra S Dittrich. Droplet microfluidics and directed evolution of enzymes: An intertwined journey. *Angew. Chem. Weinheim Bergstr. Ger.*, 133(46):24572–24591, November 2021.

[4] Maximilian Gantz, Stefanie Neun, Elliot J Medcalf, Liisa D van Vliet, and Florian Hollfelder. Ultrahigh-throughput enzyme engineering and discovery in in vitro compartments. *Chemical Reviews*, 123(9):5571–5611, May 2023.

[5] Jesse Q. Zhang, Christian A. Siltanen, Leqian Liu, Kai-Chun Chang, Zev J. Gartner, and Adam R. Abate. Linked optical and gene expression profiling of single cells at high-throughput. *Genome Biology*, 21(1):49, Feb 2020.

[6] Jinzhou Yuan, Jenny Sheng, and Peter A. Sims. Scope-seq: a scalable technology for linking live cell imaging and single-cell rna sequencing. *Genome Biology*, 19(1):227, Dec 2018.

[7] Zhouzerui Liu, Jinzhou Yuan, Anna Lasorella, Antonio Iavarone, Jeffrey N. Bruce, Peter Canoll, and Peter A. Sims. Integrating single-cell rna-seq and imaging with scope-seq2. *Scientific Reports*, 10(1):19482, Nov 2020.

[8] Fumiko Kawasaki, Yuka Mori, Takahiro Mimori, Issei Sato., and Sadao Ota. Identification of in-droplet multicellular communities by light-induced combinatorial dna barcoding. *Chemistry – A European Journal*, 29(53):e202301133, Sep 2023.

[9] Fumiko Kawasaki, Takahiro Mimori, Yuka Mori, Hiroyuki Aburatani, Nozomu Yachie, Issei Sato, and Sadao Ota. Computational design of synthetic optical barcodes in microdroplets. *Advanced Optical Materials*, 12(12):2302564, Apr 2024.

[10] Arata Tsuchida, Taikopaul Kaneko, Kaori Nishikawa, Mayu Kawasaki, Ryuji Yokokawa, and Hirofumi Shintaku. Opto-combinatorial indexing enables high-content transcriptomics by linking cell images and transcriptomes. *Lab on a Chip*, 24(8):2287–2297, 2024.

[11] Keara Lane, David Van Valen, Mialy M. DeFelice, Derek N. Macklin, Takamasa Kudo, Ariel Jaimovich, Ambrose Carr, Tobias Meyer, Dana Pe'er, Stéphane C. Boutet, and Markus W. Covert. Measuring signaling and rna-seq in the same cell links gene expression to dynamic patterns of nf-κb activation. *Cell Systems*, 4(4):458–469.e5, Apr 2017.

[12] Tyler N. Chen, Anushka Gupta, Mansi D. Zalavadia, and Aaron Streets. μcb-seq: microfluidic cell barcoding and sequencing for high-resolution imaging and sequencing of single cells. *Lab on a Chip*, 20(21):3899–3913, 2020.

[13] Johannes Bues, Joern Pezoldt, Camille Lucie Lambert, Benjamin David Hale, Elisa Bugani, Ramon Vinas Torne, Timothee Ferrari, Nadia Grenningloh, Vincent Gardeux, Shuo Wen, Caroline Wandinger, Maximilian Kohnen, Romina Augustin, Katharina Eckstein, Assia Ouanaya, Jillian Love, Sarthak Saha, Amirhossein Saba, Aviv Huttner, Maria Vittoria Impagliazzo, Jose Antonio Vasquez Porto Viso, Angel de Jesus Corria Osorio, Demetri Psaltis, Wouter Karthaus, Berend Snijder, Maria Brbic, and Bart Deplancke. Single-cell phenomics through integrated imaging and molecular profiling. *bioRxiv*, page 2025.11.28.690954, Jan 2025.

[14] Rapolas Zilionis, Juozas Nainys, Adrian Veres, Virginia Savova, David Zemmour, Allon M. Klein, and Linas Mazutis. Single-cell barcoding and sequencing using droplet microfluidics. *Nature Protocols*, 12(1):44–73, Jan 2017.

[15] Florian V. De Rop, Joy N. Ismail, Carmen Bravo González-Blas, Gert J. Hulselmans, Christopher Campbell Flerin, Jasper Janssens, Koen Theunis, Valerie M. Christiaens, Jasper Wouters, Gabriele Marcassa, Joris de Wit, Suresh Poovathingal, and Stein Aerts. Hydrop enables droplet-based single-

cell atac-seq and single-cell rna-seq using dissolvable hydrogel beads. *eLife*, 11:e73971, Feb 2022. eLife 2022;11:e73971.

[16] Paul H. Dannenberg, Jie Wang, Yue Zhuo, Sangyeon Cho, Kwon-Hyeon Kim, and Seok-Hyun Yun. Droplet microfluidic generation of a million optical microparticle barcodes. *Optics Express*, 29(23):38109–38118, Nov 2021.

[17] Yinnian Feng, Adam K. White, Jamin B. Hein, Eric A. Appel, and Polly M. Fordyce. Mrbles 2.0: High-throughput generation of chemically functionalized spectrally and magnetically encoded hydrogel beads using a simple single-layer microfluidic device. *Microsystems & Nanoengineering*, 6(1):109, Nov 2020.

[18] Daniel W. Weisgerber, Makiko Hatori, Xiangpeng Li, and Adam R. Abate. Polyhedral particles with controlled concavity by indentation templating. *Analytical Chemistry*, 94(21):7475–7482, May 2022.

[19] Sebastian Seiffert and Wilhelm Oppermann. Amine-functionalized polyacrylamide for labeling and crosslinking purposes. *Macromolecular Chemistry and Physics*, 208(16):1744–1752, Aug 2007.

[20] Byungjin Hwang, Ji Hyun Lee, and Duhee Bang. Single-cell rna sequencing technologies and bioinformaticspipelines. *Experimental & Molecular Medicine*, 50(8):1–14, Aug 2018.

[21] Hayley M. Bennett, William Stephenson, Christopher M. Rose, and Spyros Darmanis. Single-cell proteomics enabled by next-generation sequencing or mass spectrometry. *Nature Methods*, 20(3):363–374, Mar 2023.

[22] Alev Baysoy, Zhiliang Bai, Rahul Satija, and Rong Fan. The technological landscape and applications of single-cell multi-omics. *Nature Reviews Molecular Cell Biology*, 24(10):695–713, Oct 2023.

[23] Charlotte Bunne, Yusuf Roohani, Yanay Rosen, Ankit Gupta, Xikun Zhang, Marcel Roed, Theo Alexandrov, Mohammed AlQuraishi, Patricia Brennan, Daniel B Burkhardt, Andrea Califano, Jonah Cool, Abby F Dernburg, Kirsty Ewing, Emily B Fox, Matthias Haury, Amy E Herr, Eric Horvitz, Patrick D Hsu, Viren Jain, Gregory R Johnson, Thomas Kalil, David R Kelley, Shana O Kelley, Anna Kreshuk, Tim Mitchison, Stephani Otte, Jay Shendure, Nicholas J Sofroniew, Fabian Theis, Christina V Theodoris, Srigokul Upadhyayula, Marc Valer, Bo Wang, Eric Xing, Serena Yeung-Levy, Marinka

Zitnik, Theofanis Karaletsos, Aviv Regev, Emma Lundberg, Jure Leskovec, and Stephen R Quake. How to build the virtual cell with artificial intelligence: Priorities and opportunities. *Cell*, 187(25):7045–7063, December 2024.

[24] Seong-Oh Kim, Joonhui Kim, Takaharu Okajima, and Nam-Joon Cho. Mechanical properties of paraformaldehyde-treated individual cells investigated by atomic force microscopy and scanning ion conductance microscopy. *Nano Convergence*, 4(1):5, Mar 2017.

[25] Klaus Eyer, Raphaël C. L. Doineau, Carlos E. Castrillon, Luis Briseño-Roa, Vera Menrath, Guillaume Mottet, Patrick England, Alexei Godina, Elodie Brient-Litzler, Clément Nizak, Allan Jensen, Andrew D. Griffiths, Jérôme Bibette, Pierre Bruhns, and Jean Baudry. Single-cell deep phenotyping of igg-secreting cells for high-resolution immune monitoring. *Nature Biotechnology*, 35(10):977–982, Oct 2017.

[26] Gunsagar S Gulati, Jeremy Philip D'Silva, Yunhe Liu, Linghua Wang, and Aaron M Newman. Profiling cell identity and tissue architecture with single-cell and spatial transcriptomics. *Nat. Rev. Mol. Cell Biol.*, 26(1):11–31, January 2025.

[27] Marlon Stoeckius, Christoph Hafemeister, William Stephenson, Brian Houck-Loomis, Pratip K. Chattopadhyay, Harold Swerdlow, Rahul Satija, and Peter Smibert. Simultaneous epitope and transcriptome measurement in single cells. *Nature Methods*, 14(9):865–868, Sep 2017.

[28] Vanessa M. Peterson, Kelvin Xi Zhang, Namit Kumar, Jerelyn Wong, Lixia Li, Douglas C. Wilson, Renee Moore, Terrill K. McClanahan, Svetlana Sadekova, and Joel A. Klappenbach. Multiplexed quantification of proteins and transcripts in single cells. *Nature Biotechnology*, 35(10):936–939, Oct 2017.

[29] Sophia Clara Mädler, Niklas Arndt Schmacke, Alessandro Palma, Altana Namsaraeva, Ali Oğuz Can, Varvara Varlamova, Lukas Heumos, Mahima Arunkumar, Georg Wallmann, Veit Hornung, Fabian J Theis, and Matthias Mann. scportrait integrates single-cell images into multimodal modeling. September 2025.

[30] Enni Bertling, Pirta Hotulainen, Pieta K Mattila, Tanja Matilainen, Marjo Salminen, and Pekka Lappalainen. Cyclase-associated protein 1 (CAP1) pro-

motes cofilin-induced actin dynamics in mammalian nonmuscle cells. *Mol. Biol. Cell*, 15(5):2324–2334, May 2004.

[31] C Simenel, M Van Troys, J Vandekerckhove, C Ampe, and M Delepierre. Structural requirements for thymosin beta4 in its contact with actin. an NMR-analysis of thymosin beta4 mutants in solution and correlation with their biological activity. *Eur. J. Biochem.*, 267(12):3530–3538, June 2000.

[32] Marvin E Tanenbaum, Noam Stern-Ginossar, Jonathan S Weissman, and Ronald D Vale. Regulation of mRNA translation during mitosis. *Elife*, 4:e07957, August 2015.

[33] Juanjuan Zhao, Quan Yuan, Haiyan Wang, Wei Liu, Xuejiao Liao, Yingying Su, Xin Wang, Jing Yuan, Tingdong Li, Jinxiu Li, Shen Qian, Congming Hong, Fuxiang Wang, Yingxia Liu, Zhaoqin Wang, Qing He, Zhiyong Li, Bin He, Tianying Zhang, Yang Fu, Shengxiang Ge, Lei Liu, Jun Zhang, Ningshao Xia, and Zheng Zhang. Antibody responses to sars-cov-2 in patients with novel coronavirus disease 2019. *Clinical Infectious Diseases*, May 2020. ciaa344.

[34] Weilin Zeng, Yingqiu Song, Runze Wang, Rong He, and Tianlu Wang. Neutrophil elastase: From mechanisms to therapeutic potential. *J. Pharm. Anal.*, 13(4):355–366, April 2023.

[35] H Mulcahy, K P O'Rourke, C Adams, M G Molloy, and F O'Gara. LST1 and NCR3 expression in autoimmune inflammation and in response to IFN-gamma, LPS and microbial infection. *Immunogenetics*, 57(12):893–903, January 2006.

[36] Alán F Muñoz, Tim Treis, Alexandr A Kalinin, Shatavisha Dasgupta, Fabian Theis, Anne E Carpenter, and Shantanu Singh. cp_measure: API-first feature extraction for image-based profiling workflows. July 2025.

[37] Russell H. Cole, Shi-Yang Tang, Christian A. Siltanen, Payam Shahi, Jesse Q. Zhang, Sean Poust, Zev J. Gartner, and Adam R. Abate. Printed droplet microfluidics for on demand dispensing of picoliter droplets and cells. *Proceedings of the National Academy of Sciences*, 114(33):8728–8733, Aug 2017.

[38] Daniel Schraivogel, Terra M. Kuhn, Benedikt Rauscher, Marta Rodríguez-Martínez, Malte Paulsen, Keegan Owsley, Aaron Middlebrook, Christian Tischer, Beáta Ramasz, Diana Ordoñez-Rueda, Martina Dees, Sara Cuylen-

Haering, Eric Diebold, and Lars M. Steinmetz. High-speed fluorescence image–enabled cell sorting. *Science*, 375(6578):315–320, Jan 2022.

[39] Annabelle Gérard, Adam Woolfe, Guillaume Mottet, Marcel Reichen, Carlos Castrillon, Vera Menrath, Sami Ellouze, Adeline Poitou, Raphaël Doineau, Luis Briseno-Roa, Pablo Canales-Herrerias, Pascaline Mary, Gregory Rose, Charina Ortega, Matthieu Delincé, Sosthene Essono, Bin Jia, Bruno Iannascoli, Odile Richard-Le Goff, Roshan Kumar, Samantha N. Stewart, Yannick Pousse, Bingqing Shen, Kevin Grosselin, Baptiste Saudemont, Antoine Sautel-Caillé, Alexei Godina, Scott McNamara, Klaus Eyer, Gaël A. Millot, Jean Baudry, Patrick England, Clément Nizak, Allan Jensen, Andrew D. Griffiths, Pierre Bruhns, and Colin Brenan. High-throughput single-cell activity-based screening and sequencing of antibodies using droplet microfluidics. *Nature Biotechnology*, 38(6):715–721, Jun 2020.

[40] Atray Dixit, Oren Parnas, Biyu Li, Jenny Chen, Charles P. Fulco, Livnat Jerby-Arnon, Nemanja D. Marjanovic, Danielle Dionne, Tyler Burks, Raktima Raychowdhury, Britt Adamson, Thomas M. Norman, Eric S. Lander, Jonathan S. Weissman, Nir Friedman, and Aviv Regev. Perturb-seq: Dissecting molecular circuits with scalable single-cell rna profiling of pooled genetic screens. *Cell*, 167(7):1853–1866.e17, Dec 2016.

[41] Christoph Bock, Paul Datlinger, Florence Chardon, Matthew A Coelho, Matthew B Dong, Keith A Lawson, Tian Lu, Laetitia Maroc, Thomas M Norman, Bicna Song, Geoff Stanley, Sidi Chen, Mathew Garnett, Wei Li, Jason Moffat, Lei S Qi, Rebecca S Shapiro, Jay Shendure, Jonathan S Weissman, and Xiaowei Zhuang. High-content CRISPR screening. *Nat. Rev. Methods Primers*, 2(1):8, February 2022.

[42] Niklas A Schmacke, Sophia C Mädler, Georg Wallmann, Andreas Metousis, Marleen Bérouti, Hartmann Harz, Heinrich Leonhardt, Matthias Mann, and Veit Hornung. SPARCS, a platform for genome-scale CRISPR screening for spatial cellular phenotypes. June 2023.

[43] Leah C Wehmas, Susan D Hester, and Charles E Wood. Direct formalin fixation induces widespread transcriptomic effects in archival tissue samples. *Sci. Rep.*, 10(1):14497, September 2020.